Journal of Sound and Vibration (1997) **199**(3), 401–415

DYNAMIC STABILITY OF SPINNING TIMOSHENKO SHAFTS WITH A TIME-DEPENDENT SPIN RATE

H. P. Lee, T. H. Tan and G. S. B. Leng

Department of Mechanical & Production Engineering, *National University of Singapore*, 10 *Kent Ridge Crescent*, *Singapore* 119260

(*Received* 22 *August* 1995, *and in final form* 12 *June* 1996)

The equations of motion of a spinning Timoshenko shaft with time-dependent spin rate are formulated using Hamilton's principle and the assumed mode method. The deformations of the shaft are expressed in terms of an inertial reference frame. The time-dependent spin rate is assumed to be a steady state average value superimposed by sinusoidal perturbations. The resulting governing equations of motion involve periodic coefficients, which are not in the form of standard Mathieu–Hill equations. The periodic functions are embedded in both the gyroscopic and stiffness coefficient matrices. By the use of the multiple scales method, the regions of instability due to parametric excitations are determined. Numerical results for a simply supported spinning shaft are presented.

1. INTRODUCTION

Studies on the dynamic behaviour of spinning beams are related to the vibration and stability of rotating shafts, drills, end-mills, boring bars and satellite booms. A comprehensive review of this subject can be found in the publications by Dimentberg [1], Bolotin [2], Loewy and Piarulli [3], Eshleman [4], Dimaroganas and Paipeites [5] and Rao [6]. Likins *et al*. [7] and Bauer [8] investigated an Euler beam attached to a rigid base spinning with a constant angular speed. Laurenson [9] analyzed the behaviour of a spinning beam having different flexural rigidities in the two principal directions of the cross-section. Leung and Fung [10] analyzed the vibration of spinning Euler beams using the finite element method. Filipich *et al*. [11] investigated the vibration of a spinning beam with uniform cross-section having only one axis of symmetry. Lee and Jei [12] and Lee *et al*. [13] analyzed the vibration of rotating Rayleigh beams. Chen and Liao [14] reported the behaviours of spinning pre-twisted beams subjected to axial compressive loads. A consistent formulation for a rotating Timoshenko's shaft subjected to axial loads was recently reported by Choi *et al*. [15]. Zu and Han [16] presented the natural frequencies and mode shapes of spinning Timoshenko's beams with constant spin rate. Related studies on the dynamic responses of spinning shafts subjected to moving loads were reported by Huang and Chen [17] for a spinning Euler orthotropic shaft subjected to moving harmonic forces, Han and Zu [18] for a spinning Timoshenko beam with the equations of motion expressed in a body-fixed co-ordinate system, and Hashish and Sankar [19] for a spinning Timoshenko beam subjected to stationary stochastic loads using the finite element method. The spinning speed of the shafts was assumed to be constant in all of these studies. On the other hand, there have been relatively few studies on the dynamics of a spinning beam with a non-constant spin rate. Kane *et al*. [20] investigated a Timoshenko beam built into

0022–460X/97/030401 + 15 $25.00/0/sv960656

a rigid base undergoing general three-dimensional motions. Kammer and Schlack [21] analyzed an Euler beam with a constant spin rate superimposed by small periodic perturbations using a KBM perturbation method. The stability of a spinning Timoshenko beam with a time-dependent spin rate has not been analyzed.

The equations of motion of a spinning Euler beam with circular cross-section, when derived in an inertial co-ordinate system, have been shown to be identical to the equation of motion of a non-spinning Euler beam (see, for example, Han and Zu [18]). The behaviour of a spinning Euler beam with a circular cross-section is therefore independent of the spinning speed. A spinning Euler beam with equal flexural rigidities in the two principal directions of the cross-section was also reported by Kammer and Schlack [21] to be always stable, independent of the spinning speed. More recently, a few publications, including those by Young and Liou [22, 23] as well as by Liao and Huang [24, 25], make use of a modal analysis technique developed by Meirovitch [26] to uncouple the equations of motion of gyroscopic systems. Subsequently, the multiple scales method is applied to perform the parametric analysis. Their equations of motion are formulated based on Euler's beam model.

When the equations of motion of a spinning Timoshenko shaft are derived in an inertial frame of reference, the spinning speed of the shaft appears in the equations of motion (see, for example, Chen and Ku [27]). The stability of the shaft is therefore expected to be dependent on the spinning speed. These equations of motion in matrix form are formulated in the present study using Hamilton's principle and the assumed mode method for a spinning shaft with time-dependent spin rate. The deformations of the shaft are expressed in an inertial reference frame. The spinning speed of the shaft is assumed to be a steady state average value, on which sinusoidal perturbations are superimposed. The resulting equations of motion are found to be different from the standard Mathieu–Hill equations, and this form of equation has not been analyzed in the literature. This coupled set of equations of motion is then uncoupled and the multiple scales method is used to determine the instability boundaries of the system. Numerical results are presented for a simply supported spinning Timoshenko shaft.

2. THEORY AND FORMULATION

The shaft considered is an axisymmetric shaft of uniform circular cross-section and length L, rotating about its longitudinal axis and simply supported at its two ends, shown in Figure 1. A set of co-ordinates (X, Y, Z) is assumed to be fixed in an inertial frame, with the X-axis parallel to the undeformed longitudinal axis of the rotating shaft. The shaft is assumed to be spinning with a time dependent rotational speed, denoted by Ω. The deformation of the shaft is assumed to be governed by Timoshenko's beam theory. The deformed state of the shaft can be described by the transverse translations $V(s, t)$ and $W(s, t)$ in the Y and Z directions and by small angular displacements $B(s, t)$ and $\Gamma(s, t)$ about the Y- and Z-axes. The variable s is the position of a point along the beam on the X-axis and t is the time. The two translations V and W consist of contributions due to bending, V_b and W_b, and contributions due to transverse shear deformation, V_s and W_s. The relations amongst these variables are as follows [27]:

$$V(s, t) = V_b(s, t) + V_s(s, t), \qquad W(s, t) = W_b(s, t) + W_s(s, t) \tag{1, 2}$$

$$B(s, t) = -\partial W_b(s, t)/\partial s, \qquad \Gamma(s, t) = \partial V_b(s, t)/\partial s. \tag{3, 4}$$

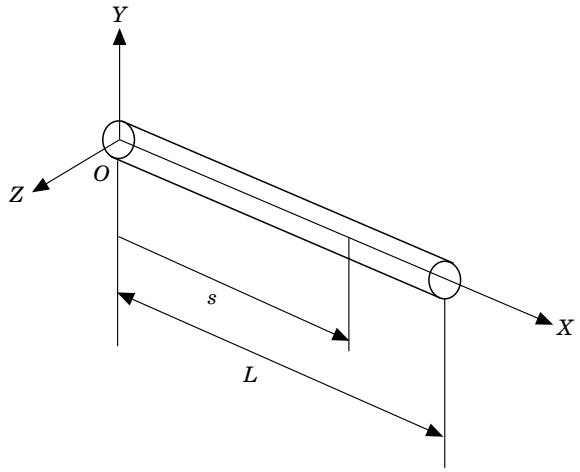

Figure 1. A spinning Timoshenko shaft subjected to a time-dependent spin speed.

The potential energy, U, of the beam due to elastic bending and shear deformation is given by Chen and Ku [27] as

$$U = \tfrac{1}{2}\int_0^L EI\{(V_b'')^2 + (W_b'')^2\}\,\mathrm{d}s + \tfrac{1}{2}\int_0^L kGA\{(V_s')^2 + (W_s')^2\}\,\mathrm{d}s, \tag{5}$$

where the prime ($'$) denotes partial differentiation with respect to s. The parameter E is Young's modulus, G is the shear modulus, k is the shear coefficient, I is the second moment of area, and A is the cross-sectional area of the shaft. Using the relations between the rotational and translational variables, the above expression can be rearranged as

$$U = \tfrac{1}{2}\int_0^L EI\{(\Gamma')^2 + (B')^2\}\,\mathrm{d}s + \tfrac{1}{2}\int_0^L kGA\{(V')^2 + (W') + \Gamma^2 + B^2 - 2\Gamma V' + 2BW'\}\,\mathrm{d}s. \tag{6}$$

Similarly, the kinetic energy T of the beam as given in Chen and Ku [27] is

$$T = \tfrac{1}{2}\int_0^L \rho A\{(\dot{V})^2 + (\dot{W})^2\}\,\mathrm{d}s + \tfrac{1}{2}\int_0^L I_d\{(\dot{B})^2 + (\dot{\Gamma})^2\}\,\mathrm{d}s - \tfrac{1}{2} I_p\Omega\int_0^L \{\dot{\Gamma}B - \dot{B}\Gamma\}\,\mathrm{d}s + \tfrac{1}{2}\Omega^2\int_0^L I_p\,\mathrm{d}s, \tag{7}$$

where the dot ($\dot{}$) denotes differentiation with respect to time. The variable ρ is the mass density of the shaft, and I_d and I_p are the diametral and polar mass moments of inertia of the shaft per unit length.

Using the assumed mode method, the quantities V, W, Γ and B can be expressed as

$$V(s,t) = \sum_{i=1}^{n} v_i(t)\phi_i(s), \qquad W(s,t) = \sum_{i=1}^{n} w_i(t)\phi_i(s), \tag{8, 9}$$

$$B(s,t) = \sum_{i=1}^{n} p_i(t)\psi_i(s), \qquad \Gamma(s,t) = \sum_{i=1}^{n} q_i(t)\psi_i(s), \tag{10, 11}$$

where ϕ_i and ψ_i are spatial functions that satisfy the boundary conditions at the two ends of the shaft. For a shaft simply supported at both ends, these assumed functions are as follows:

$$\phi_i(s) = \sqrt{2}\sin\frac{i\pi s}{L}, \qquad \psi_i(s) = \sqrt{2}\cos\frac{i\pi s}{L}. \tag{12, 13}$$

The assumed forms of V, W, Γ and B enable the kinetic energy and the potential energy to be expressed in matrix form as follows:

$$T = \tfrac{1}{2}\rho A\dot{\mathbf{v}}^{\mathrm{T}}\mathbf{M}\dot{\mathbf{v}} + \tfrac{1}{2}\rho A\dot{\mathbf{w}}^{\mathrm{T}}\mathbf{M}\dot{\mathbf{w}} + \tfrac{1}{2}I_d\dot{\mathbf{p}}^{\mathrm{T}}\mathbf{S}\dot{\mathbf{p}} + \tfrac{1}{2}I_d\dot{\mathbf{q}}^{\mathrm{T}}\mathbf{S}\dot{\mathbf{q}} - \tfrac{1}{2}\Omega I_p\dot{\mathbf{q}}^{\mathrm{T}}\mathbf{S}\mathbf{p} + \tfrac{1}{2}\Omega I_p\dot{\mathbf{p}}^{\mathrm{T}}\mathbf{S}\mathbf{q} + \tfrac{1}{2}\Omega^2\int_0^L I_p\,\mathrm{d}s, \tag{14}$$

$$U = \tfrac{1}{2}EI\mathbf{p}^{\mathrm{T}}\mathbf{K}\mathbf{p} + \tfrac{1}{2}EI\mathbf{q}^{\mathrm{T}}\mathbf{K}\mathbf{q} + \tfrac{1}{2}kGA\mathbf{v}^{\mathrm{T}}\mathbf{H}\mathbf{v} + \tfrac{1}{2}kGA\mathbf{w}^{\mathrm{T}}\mathbf{H}\mathbf{w} + \tfrac{1}{2}kGA\mathbf{p}^{\mathrm{T}}\mathbf{S}\mathbf{p} + \tfrac{1}{2}kGA\mathbf{q}^{\mathrm{T}}\mathbf{S}\mathbf{q} - kGA\mathbf{q}^{\mathrm{T}}\mathbf{E}\mathbf{v} + kGA\mathbf{p}^{\mathrm{T}}\mathbf{E}\mathbf{w}. \tag{15}$$

where $\mathbf{M}$, $\mathbf{S}$, $\mathbf{K}$, $\mathbf{H}$ and $\mathbf{E}$ are matrices, defined as

$$(\mathbf{M})_{ij} = \int_0^L \phi_i\phi_j\,\mathrm{d}s, \qquad (\mathbf{S})_{ij} = \int_0^L \psi_i\psi_j\,\mathrm{d}s, \qquad (\mathbf{K})_{ij} = \int_0^L \psi_i'\psi_j'\,\mathrm{d}s, \tag{16–18}$$

$$(\mathbf{H})_{ij} = \int_0^L \phi_i'\phi_j'\,\mathrm{d}s, \qquad (\mathbf{E})_{ij} = \int_0^L \psi_i\phi_j'\,\mathrm{d}s. \tag{19, 20}$$

The vectors $\mathbf{v}$ and $\dot{\mathbf{v}}$ are $n \times 1$ column vectors consisting of v_i and $\dot{v}_i$ respectively. The other vectors are also defined in a similar manner.

The Lagrangian of the rotating shaft can be expressed as

$$\mathscr{L} = T - U. \tag{21}$$

Using Hamilton's principle, the resulting Euler–Langrange equations are

$$\rho A\mathbf{M}\ddot{\mathbf{v}} + kGA\mathbf{H}\mathbf{v} - kGA\mathbf{E}^{\mathrm{T}}\mathbf{q} = \mathbf{0}, \qquad \rho A\mathbf{M}\ddot{\mathbf{w}} + kGA\mathbf{H}\mathbf{w} + kGA\mathbf{E}^{\mathrm{T}}\mathbf{p} = \mathbf{0}, \tag{22, 23}$$

$$I_d\mathbf{S}\ddot{\mathbf{p}} + \Omega I_p\mathbf{S}\dot{\mathbf{q}} + EI\mathbf{K}\mathbf{p} + kGA\mathbf{S}\mathbf{p} + kGA\mathbf{E}\mathbf{w} + \tfrac{1}{2}\dot{\Omega}I_p\mathbf{S}\mathbf{q} = \mathbf{0}, \tag{24}$$

$$I_d\mathbf{S}\ddot{\mathbf{q}} - \Omega I_p\mathbf{S}\dot{\mathbf{p}} + EI\mathbf{K}\mathbf{q} + kGA\mathbf{S}\mathbf{q} - kGA\mathbf{E}\mathbf{v} - \tfrac{1}{2}\dot{\Omega}I_p\mathbf{S}\mathbf{p} = \mathbf{0}. \tag{25}$$

Non-dimensionalization can be carried out by introducing the following dimensionless variables:

$$\tau = t\sqrt{G/\rho L^2}, \qquad \bar{\Omega} = \Omega\sqrt{\rho L^2/G}, \qquad \xi = s/L, \qquad \bar{v} = v/L, \qquad \bar{w} = w/L, \qquad \bar{p} = p,$$

$$\bar{q} = q, \qquad \bar{I}_d = I_d/\rho A L^2 = (\beta/\pi)^2, \qquad \bar{I}_p = I_p/\rho A L^2 = 2(\beta/\pi)^2,$$

$$\mu = \frac{EI}{GAL^2} = \frac{2I(1+\nu)}{AL^2} = 2(1+\nu)\left(\frac{r_0}{L}\right)^2 = 2(1+\nu)\left(\frac{\beta}{\pi}\right)^2, \tag{26}$$

where the radius of gyration $r_0 = \sqrt{I/A}$, Rayleigh's coefficient $\beta = \pi r_0/L$ and, by assuming isotropic material, E and G can be linked via the Poisson ratio using $G = E/2(1+\nu)$.

$$\bar{\mathbf{M}}\ddot{\bar{\mathbf{v}}} + k\bar{\mathbf{H}}\bar{\mathbf{v}} - k\bar{\mathbf{E}}^{\mathrm{T}}\bar{\mathbf{q}} = \mathbf{0}, \tag{27}$$

$$\bar{\mathbf{M}}\ddot{\bar{\mathbf{w}}} + k\bar{\mathbf{H}}\bar{\mathbf{w}} + k\bar{\mathbf{E}}^{\mathrm{T}}\bar{\mathbf{p}} = \mathbf{0}, \tag{28}$$

$$\bar{I}_d\bar{\mathbf{S}}\ddot{\bar{\mathbf{p}}} + \bar{\Omega}\bar{I}_p\bar{\mathbf{S}}\dot{\bar{\mathbf{q}}} + \mu\bar{\mathbf{K}}\bar{\mathbf{p}} + k\bar{\mathbf{S}}\bar{\mathbf{p}} + k\bar{\mathbf{E}}\bar{\mathbf{w}} + \tfrac{1}{2}\dot{\bar{\Omega}}\bar{I}_p\bar{\mathbf{S}}\bar{\mathbf{q}} = \mathbf{0}, \tag{29}$$

$$\bar{I}_d\bar{\mathbf{S}}\ddot{\bar{\mathbf{q}}} - \bar{\Omega}\bar{I}_p\bar{\mathbf{S}}\dot{\bar{\mathbf{p}}} + \mu\bar{\mathbf{K}}\bar{\mathbf{q}} + k\bar{\mathbf{S}}\bar{\mathbf{q}} - k\bar{\mathbf{E}}\bar{\mathbf{v}} - \tfrac{1}{2}\dot{\bar{\Omega}}\bar{I}_p\bar{\mathbf{S}}\bar{\mathbf{p}} = \mathbf{0}. \tag{30}$$

The above are coupled second order differential equations which can be combined to give

$$\mathbf{M}_0\ddot{\mathbf{a}} + \bar{\Omega}\mathbf{M}_1\dot{\mathbf{a}} + (\mathbf{M}_2 + \tfrac{1}{2}\dot{\bar{\Omega}}\mathbf{M}_1)\mathbf{a} = \mathbf{0}. \tag{31}$$

The vector $\mathbf{a}$ is a $4n \times 1$ column vector, defined as $\mathbf{a} = (\mathbf{v}\ \mathbf{w}\ \mathbf{p}\ \mathbf{q})^{\mathrm{T}}$, whereas the other matrices are as follows:

$$\mathbf{M}_0 = \begin{bmatrix} \bar{\mathbf{M}} & \mathbf{0} & \mathbf{0} & \mathbf{0} \\ \mathbf{0} & \bar{\mathbf{M}} & \mathbf{0} & \mathbf{0} \\ \mathbf{0} & \mathbf{0} & \bar{I}_d\bar{\mathbf{S}} & \mathbf{0} \\ \mathbf{0} & \mathbf{0} & \mathbf{0} & \bar{I}_d\bar{\mathbf{S}} \end{bmatrix}, \qquad \mathbf{M}_1 = \begin{bmatrix} \mathbf{0} & \mathbf{0} & \mathbf{0} & \mathbf{0} \\ \mathbf{0} & \mathbf{0} & \mathbf{0} & \mathbf{0} \\ \mathbf{0} & \mathbf{0} & \mathbf{0} & \bar{I}_p\bar{\mathbf{S}} \\ \mathbf{0} & \mathbf{0} & -\bar{I}_p\bar{\mathbf{S}} & \mathbf{0} \end{bmatrix},$$

$$\mathbf{M}_2 = \begin{bmatrix} k\bar{\mathbf{H}} & \mathbf{0} & \mathbf{0} & -k\bar{\mathbf{E}}^{\mathrm{T}} \\ \mathbf{0} & k\bar{\mathbf{H}} & k\bar{\mathbf{E}}^{\mathrm{T}} & \mathbf{0} \\ \mathbf{0} & k\bar{\mathbf{E}} & \mu\bar{\mathbf{K}} + k\bar{\mathbf{S}} & \mathbf{0} \\ -k\mathbf{E} & \mathbf{0} & \mathbf{0} & \mu\bar{\mathbf{K}} + k\bar{\mathbf{S}} \end{bmatrix}.$$

The non-zero quantity $\dot{\bar{\Omega}}$ is the dimensionless angular acceleration of the spinning shaft arising from the time-dependency of the spinning speed. The dimensionless spinning speed $\bar{\Omega}$ is assumed to be a steady state value Ω_0 on which is superimposed a harmonic perturbation of amplitude Ω_p and a dimensionless frequency of perturbation ω:

$$\bar{\Omega} = \Omega_0 + \Omega_p \cos\omega\tau. \tag{32}$$

Therefore, equation (31) can be rewritten as

$$\mathbf{M}_0\ddot{\mathbf{a}} + (\Omega_0 + \Omega_p\cos\omega\tau)\mathbf{M}_1\dot{\mathbf{a}} + \left(\mathbf{M}_2 - \frac{\Omega_p\omega\sin\omega\tau}{2}\mathbf{M}_1\right)\mathbf{a} = \mathbf{0}. \tag{33}$$

The equation of motion is not in the form of the standard Mathieu–Hill equation due to the additional time dependent coefficient of the $\dot{\mathbf{a}}$ term. Pre-multiplying the entire equation (33) by $\mathbf{M}_0^{-1}$ and introducing $\Omega_p = \varepsilon\Omega_0$, it can be transformed into

$$\ddot{\mathbf{a}} + \Omega_0(1 + \varepsilon \cos \omega\tau)\mathbf{M}_0^{-1}\mathbf{M}_1\dot{\mathbf{a}} + \left(\mathbf{M}_0^{-1}\mathbf{M}_2 - \frac{\varepsilon\Omega_0\omega \sin \omega\tau}{2}\mathbf{M}_0^{-1}\mathbf{M}_1\right)\mathbf{a} = \mathbf{0}. \tag{34}$$

Equation (34) is a set of differential equations which cannot be solved directly. The modal analysis procedure used for uncoupling this gyroscopic system is similar to that used by Meirovitch [26]. First we define a state vector $\mathbf{b} = [\dot{\mathbf{a}}, \mathbf{a}]^{\mathrm{T}}$ and rewrite equation (34) as

$$\dot{\mathbf{b}} - \mathbf{KKb} = \tfrac{1}{2}\varepsilon\Omega_0\omega \sin \omega\tau\mathbf{F1b} - \varepsilon\Omega_0 \cos \omega\tau\mathbf{F2b}, \tag{35}$$

where

$$\mathbf{KK} = \begin{bmatrix} -\Omega_0\mathbf{M}_0^{-1}\mathbf{M}_1 & -\mathbf{M}_0^{-1}\mathbf{M}_2 \\ \mathbf{I} & \mathbf{0} \end{bmatrix}, \qquad \mathbf{F1} = \begin{bmatrix} \mathbf{0} & \mathbf{M}_0^{-1}\mathbf{M}_1 \\ \mathbf{0} & \mathbf{0} \end{bmatrix}, \qquad \mathbf{F2} = \begin{bmatrix} \mathbf{M}_0^{-1}\mathbf{M}_1 & \mathbf{0} \\ \mathbf{0} & \mathbf{0} \end{bmatrix}.$$

The eigenvalues of the above system come in conjugate pairs of pure imaginary numbers ($\pm \mathrm{i}\omega_i$) which are the natural frequencies of the gyroscopic system (note that $\mathrm{i} = \sqrt{-1}$, whereas subscript i represents the ith mode). The modal matrix $\mathbf{P}$ is formed by assembling the real and imaginary parts of the corresponding normalized eigenvectors of the transformed stiffness matrix. The substitution of a linearly transformed $\mathbf{b} = \mathbf{P}\boldsymbol{\zeta}$, followed by pre-multiplication of $\mathbf{P}^{-1}$ with equation (35) yields

$$\dot{\boldsymbol{\zeta}} - \boldsymbol{\Lambda}\boldsymbol{\zeta} = \varepsilon\Omega_0\left(\frac{\omega}{2} \sin \omega\tau\mathbf{FS} - \cos \omega\tau\mathbf{FC}\right)\boldsymbol{\zeta}, \tag{36}$$

where

$$\boldsymbol{\Lambda} = \mathbf{P}^{-1}\mathbf{KKP}, \qquad \mathbf{FS} = \mathbf{P}^{-1}\mathbf{F1P}, \qquad \mathbf{FC} = \mathbf{P}^{-1}\mathbf{F2P}. \tag{37}$$

$\boldsymbol{\Lambda}$ is a real matrix with 2×2 blocks of

$$\begin{bmatrix} 0 & +\omega_i \\ -\omega_i & 0 \end{bmatrix}$$

along its diagonal, instead of having the purely imaginary eigenvalues along its diagonal.

Although the left side of this set of equations is uncoupled in the block sense, the terms on the right side remain uncoupled. In order to match the structure of $\boldsymbol{\Lambda}$, the transformed state vector is chosen to be of the following form

$$\boldsymbol{\zeta} = [\xi_1, \eta_1, \xi_2, \eta_2, \ldots \xi_i, \eta_i, \ldots \xi_m, \eta_m]^{\mathrm{T}},$$

where $m = 4n$. A general pair of discrete equations from equation (36) can be written as

$$\xi_i - \omega_i\eta_i = \tfrac{1}{2}\varepsilon\Omega_0\omega\left(\sum_{j=1}^{m}(fs_{2i-1,2j-1}\xi_j + fs_{2i-1,2j}\eta_j)\right) \sin \omega\tau$$

$$- \varepsilon\Omega_0\left(\sum_{j=1}^{m}(fc_{2i-1,j-1}\xi_j + fc_{2i-1,2j}\eta_j)\right) \cos \omega\tau,$$

$$\eta_i + \omega_i \xi_i = \tfrac{1}{2}\varepsilon\Omega_0\omega\left(\sum_{j=1}^{m} (fs_{2i,2j-1}\xi_j + fs_{2i,2j}\eta_j)\right)\sin\omega\tau$$

$$-\varepsilon\Omega_0\left(\sum_{j=1}^{m} (fc_{2i,2j-1}\xi_j + fc_{2i,2j}\eta_j)\right)\cos\omega\tau. \tag{38}$$

In the multiple scales method, ξ_i and η_i are assumed to be of the form

$$\xi_i(\tau) = \xi_{i(0)}(T_0, T_1, T_2, \ldots) + \varepsilon\xi_{i(1)}(T_0, T_1, T_2, \ldots) + \varepsilon^2\xi_{i(2)}(T_0, T_1, T_2, \ldots) + \cdots,$$

$$\eta_i(\tau) = \eta_{i(0)}(T_0, T_1, T_2, \ldots) + \varepsilon\eta_{i(1)}(T_0, T_1, T_2, \ldots) + \varepsilon^2\eta_{i(2)}(T_0, T_1, T_2, \ldots) + \cdots,$$

$$\text{for } i = 1, 2, \ldots, m, \tag{39}$$

where i is the mode number and each term is a function of a set of independent variables T_r, defined as $\varepsilon^r\tau$, for $r = 0, 1, \ldots, M$. Among the recent publications [22]–[25] that utilize Meirovitch's modal analysis technique for a gyroscopic system followed by the multiple scales method, only Young and Liou [23] went beyond $M = 2$. However, in their plate analysis, the range of ε goes from 0·0 to 1·0 and yet the presented graphical results only show minute difference between the first and second order resonances. Given the present range of ε from 0·0 to 0·1, the results of *perturbation* analysis obtained using the multiple scales method with first order uniform expansion should be sufficient. With $M = 2$, only T_0 and T_1 will be required. Detail discussions on the multiple scales method can be found in reference [25]. Upon substitution of equation (39) into equation (38), gathering coefficients of like powers of ε yields the following equations:

order 0 (ε^0),
$$D_0\xi_{i(0)} - \omega_i\eta_{i(0)} = 0, \qquad D_0\eta_{i(0)} + \omega_i\xi_{i(0)} = 0; \tag{40}$$

order 1 (ε^1),

$$D_0\xi_{i(1)} - \omega_i\eta_{i(1)} = -D_1\xi_{i(0)} + \tfrac{1}{2}\Omega_0\omega\left(\sum_{j=1}^{m} (fs_{2i-1,2j-1}\xi_{j(0)} + fs_{2i-1,2j}\eta_{j(0)})\right)\sin\omega\tau$$

$$-\Omega_0\left(\sum_{j=1}^{m} (fc_{2i-1,2j-1}\xi_{j(0)} + fc_{2i-1,2j}\eta_{j(0)})\right)\cos\omega\tau,$$

$$D_0\eta_{i(1)} + \omega_i\xi_{i(1)} = -D_1\eta_{i(0)} + \tfrac{1}{2}\Omega_0\omega\left(\sum_{j=1}^{m} (fs_{2i,2j-1}\xi_{j(0)} + fs_{2i,2j}\eta_{j(0)})\right)\sin\omega\tau$$

$$-\Omega_0\left(\sum_{j=1}^{m} (fc_{2i,2j-1}\xi_{j(0)} + fc_{2i,2j}\eta_{j(0)})\right)\cos\omega\tau. \tag{41}$$

Solving equation (40) yields a pair of general solutions, given by

$$\xi_{i(0)} = A_i(T_1)\,\mathrm{e}^{\mathrm{i}\omega_i T_0} + \bar{A}_i(T_1)\,\mathrm{e}^{-\mathrm{i}\omega_i T_0}, \qquad \eta_{i(0)} = \mathrm{i}A_i(T_1)\,\mathrm{e}^{\mathrm{i}\omega_i T_0} - \mathrm{i}\bar{A}_1(T_1)\,\mathrm{e}^{-\mathrm{i}\omega_i T_0}. \tag{42}$$

Each of these solutions comprises two terms, in which the second is the complex conjugate of the first. All of the coefficients are undetermined functions of T_1. Substituting this pair

of equations and its differentials into equation (41) with the trigonometric functions reexpressed in exponential form yields

$$
\begin{aligned}
D_0\xi_{i(1)} - \omega_i\eta_{i(1)} = {} & -A_i' \, e^{i\omega_i T_0} - \bar{A}_i' \, e^{-i\omega_i T_0} - \frac{i\Omega_0\omega}{4} \sum_{j=1}^{m} \{ fs_{2i-1,2j-1}[A_j \, e^{i(\omega+\omega_j)T_0} \\
& + \bar{A}_j \, e^{i(\omega-\omega_j)T_0}] + ifs_{2i-1,2j}[A_j \, e^{i(\omega+\omega_j)T_0} - \bar{A}_j \, e^{i(\omega-\omega_j)T_0}] \\
& - fs_{2i-1,2j-1}[A_j \, e^{-i(\omega-\omega_j)T_0} + \bar{A}_j \, e^{-i(\omega+\omega_j)T_0}] \\
& - ifs_{2i-1,2j}[A_j \, e^{-i(\omega-\omega_j)T_0} - \bar{A}_j \, e^{-i(\omega+\omega_j)T_0}]\} \\
& - \frac{\Omega_0}{2} \sum_{j=1}^{m} \{ fc_{2i-1,2j-1}[A_j \, e^{i(w+\omega_j)T_0} + \bar{A}_j \, e^{i(\omega-\omega_j)T_0}] \\
& + ifc_{2i-1,2j}[A_j \, e^{i(\omega+\omega_j)T_0} - \bar{A}_j \, e^{i(\omega-\omega_j)T_0}] \\
& + fc_{2i-1,2j-1}[A_j \, e^{-i(\omega-\omega_j)T_0} + \bar{A}_j \, e^{-i(\omega+\omega_j)T_0}] \\
& + ifc_{2i-1,2j}[A_j \, e^{-i(\omega-\omega_j)T_0} - \bar{A}_j \, e^{-i(\omega+\omega_j)T_0}]\},
\end{aligned}
$$

$$
\begin{aligned}
D_0\eta_{i(1)} + \omega_i\xi_{i(1)} = {} & -iA_i' \, e^{i\omega_i T_0} + i\bar{A}_i' \, e^{-i\omega_i T_0} - \frac{i\Omega_0\omega}{4} \sum_{j=1}^{m} \{ fs_{2i,2j-1}[A_j \, e^{i(\omega+\omega_j)T_0} \\
& + \bar{A}_j \, e^{i(\omega-\omega_j)T_0}] + ifs_{2i,2j}[A_j \, e^{i(\omega+\omega_j)T_0} - \bar{A}_j \, e^{i(\omega-\omega_j)T_0}] \\
& - fs_{2i,2j-1}[A_j \, e^{-i(\omega-\omega_j)T_0} - \bar{A}_j \, e^{-i(\omega+\omega_j)T_0}] \\
& - ifs_{2i,2j}[A_j \, e^{-i(\omega-\omega_j)T_0} - \bar{A}_j \, e^{-i(\omega+\omega_j)T_0}]\} - \frac{\Omega_0}{2} \sum_{j=1}^{m} \{ fc_{2i,2j-1}[A_j \, e^{i(\omega+\omega_j)T_0} \\
& + \bar{A}_j \, e^{i(\omega-\omega_j)T_0}] + ifc_{2i,2j}[A_j \, e^{i(\omega+\omega_j)T_0} - \bar{A}_j \, e^{i(\omega-\omega_j)T_0}] \\
& + fc_{2i,2j-1}[A_j \, e^{-i(\omega-\omega_j)T_0} + \bar{A}_j \, e^{-i(\omega+\omega_j)T_0}] + ifc_{2i,2j}[A_j \, e^{-i(\omega-\omega_j)T_0} \\
& - \bar{A}_j \, e^{-i(\omega+\omega_j)T_0}]\}. \qquad (43)
\end{aligned}
$$

The general solution of this pair of equations is of the same form as that given in equation (42). Before attempting to solve for the particular solutions of $\xi_{i(1)}$ and $\eta_{i(1)}$, we need to check if the frequency of perturbation (ω) is far from or near to the individual frequencies, as well as to their combination. The focus in this case is on the sum-type resonance, which also includes superharmonic resonance due to $2\omega_i$.

2.1. ω FAR FROM $\omega_p + \omega_q$

When the perturbation frequency ω is far from the combinations of its natural frequencies, terms that can give rise to secular terms will not surface. Hence particular solutions with decaying exponents can be obtained for periodic inputs and the system is said to be stable. A similar situation was encountered by Young and Liou [22] and Liao and Huang [25] when their systems were subjected to time-dependent spinning speed.

2.2. ω NEAR $\omega_p + \omega_q$

However, as the perturbation frequency ω approaches the sum of any two natural frequencies of the system, combinational resonance of the summed-type can occur. Superharmonic resonance due to ω approaching $2\omega_i$ will also be presented if they exist.

A quantitative study on the dynamic stability of the system can be carried out by relating ω to the natural frequencies of any two modes, ω_p and ω_q; i.e.,

$$\omega = \omega_p + \omega_q + \sigma\varepsilon, \tag{44}$$

where σ is a detuning factor to describe the nearness. Substitution of equation (44) into equation (43) results in the emergence of the undesirable secular term $e^{i\omega_p T_0}$, or $e^{i\omega_q T_0}$. The particular solutions can be obtained by expressing $\xi_{i(1),p}$ and $\eta_{i(1),p}$ as

$$\xi_{i(1),p} = B_{i1}(T_1)\, e^{i\omega_i T_0} \qquad \text{and} \qquad \eta_{i(1),p} = B_{i2}(T_1)\, e^{i\omega_i T_0}. \tag{45}$$

Upon substitution of equation (45) into equation (43), and equating the coefficient of $e^{+i\omega_p T_0}$ to zero ($i = p$ and $j = q$), the following pair of equations with a singular coefficient matrix is obtained:

$$\begin{aligned}
i\omega_p B_{p1} - \omega_p B_{p2} = {} & -A_p' - \frac{i\Omega_0\omega}{4}\left[(fs_{2p-1,2q-1} - ifs_{2p-1,2q})\bar{A}_q\, e^{i\sigma T_1}\right] \\
& - \frac{\Omega_0}{2}\left[(fc_{2p-1,2q-1} - ifc_{2p-1,2q})\bar{A}_q\, e^{i\sigma T_1}\right], \\
\omega_p B_{p1} + i\omega_p B_{p2} = {} & -iA_p' - \frac{i\Omega_0\omega}{4}\left[(fs_{2p,2q-1} - ifs_{2p,2q})\bar{A}_q\, e^{i\sigma T_1}\right] \\
& - \frac{\Omega_0}{2}\left[(fc_{2p,2q-1} - ifc_{2p,2q})\bar{A}_q\, e^{i\sigma T_1}\right].
\end{aligned} \tag{46}$$

Let us denote the right sides of equation (46) by R_{p1} and R_{p2} to reduce the tedious algebra. The solutions for B_{p1} and B_{p2} will only exist if

$$\begin{vmatrix} i\omega_p & R_{p1} \\ \omega_p & R_{p2} \end{vmatrix} = 0. \tag{47}$$

When $i = q$ and $j = p$, equating the coefficient of $e^{-i\omega_q T_0}$ to zero yields

$$\begin{aligned}
i\omega_q B_{q1} - \omega_q B_{q2} = {} & -A_q' - \frac{i\Omega_0\omega}{4}\left[(fs_{2q-1,2p-1} - ifs_{2q-1,2p})\bar{A}_p\, e^{i\sigma T_1}\right] \\
& - \frac{\Omega_0}{2}\left[(fc_{2q-1,2p-1} - ifc_{2q-1,2p})\bar{A}_p\, e^{i\sigma T_1}\right], \\
\omega_q B_{q1} + i\omega_q B_{q2} = {} & -iA_q' - \frac{i\Omega_0\omega}{4}\left[(fs_{2q,2p-1} - ifs_{2q,2p})\bar{A}_p\, e^{i\sigma T_1}\right] \\
& - \frac{\Omega_0}{2}\left[(fc_{2q,2p-1} - ifc_{2q,2p})\bar{A}_p\, e^{i\sigma T_1}\right].
\end{aligned} \tag{48}$$

Denoting the right sides by R_{q1} and R_{q2} results in the following simplified forms:

$$i\omega_q B_{q1} - \omega_q B_{q2} = R_{q1}, \qquad \omega_q B_{q1} + i\omega_q B_{q2} = R_{q2}.$$

The solutions for B_{q1} and B_{q2} will only exist if

$$\begin{vmatrix} \mathrm{i}\omega_q & R_{q1} \\ \omega_q & R_{q2} \end{vmatrix} = 0. \tag{49}$$

Rewriting equation (47) and taking the conjugate of the left side of equation (49),

$$D_1 A_p + \Lambda_{pq} \bar{A}_q \, \mathrm{e}^{\mathrm{i}\sigma T_1} = 0, \qquad D_1 \bar{A}_q + \bar{\Lambda}_{qp} A_p \, \mathrm{e}^{-\mathrm{i}\sigma T_1} = 0, \tag{50}$$

where

$$\Lambda_{pq} = \frac{\Omega_0}{4} \left\{ \frac{\omega}{2} [(fs_{2p,2q-1} + fs_{2p-1,2q}) + \mathrm{i}(fs_{2p-1,2q-1} - fs_{2p,2q})] + (fc_{2p-1,2q-1} - fc_{2p,2q}) \right.$$

$$\left. - \mathrm{i}(fc_{2p,2q-1} + fc_{2p-1,2q}) \right\},$$

$$\bar{\Lambda}_{qp} = \frac{\Omega_0}{4} \left\{ \frac{\omega}{2} [(fs_{2q,2p-1} + fs_{2q-1,2p}) - \mathrm{i}(fs_{2q-1,2p-1} - fs_{2q,2p})] + (fc_{2q-1,2p-1} - fc_{2q,2p}) \right.$$

$$\left. + \mathrm{i}(fc_{2q,2p-1} + fc_{2q-1,2p}) \right\}. \tag{51}$$

Let us assume the solutions of equation (50) to be of the forms

$$A_p = E_p(T_2) \, \mathrm{e}^{-\mathrm{i}\lambda T_1} \qquad \text{and} \qquad \bar{A}_q = \bar{E}_q(T_2) \, \mathrm{e}^{-\mathrm{i}(\lambda+\sigma)T_1}, \tag{52}$$

where $E_p(T_2)$ and $\bar{E}_q(T_2)$ are complex functions, while $\bar{\lambda}$ is the complex conjugate of λ. Substituting equation (52) into equation (50) yields the following matrix equation:

$$\begin{bmatrix} -\mathrm{i}\lambda \, \mathrm{e}^{-\mathrm{i}\lambda T_1} & \Lambda_{pq} \, \mathrm{e}^{-\mathrm{i}\lambda T_1} \\ \bar{\Lambda}_{qp} \, \mathrm{e}^{-\mathrm{i}(\lambda+\sigma)T_1} & -\mathrm{i}(\lambda+\sigma) \, \mathrm{e}^{-\mathrm{i}(\lambda+\sigma)T_1} \end{bmatrix} \begin{bmatrix} E_p \\ \bar{E}_q \end{bmatrix} = \begin{bmatrix} 0 \\ 0 \end{bmatrix}. \tag{53}$$

For a non-trivial solution, the determinant of the 2×2 matrix must be zero, i.e.,

$$\lambda = \tfrac{1}{2}(-\sigma \pm \sqrt{\sigma^2 - 4\Lambda_{pq}\bar{\Lambda}_{qp}}). \tag{54}$$

Since the system is stable only when the imaginary part of λ is negative, the transition at which $\mathrm{Im}\,(\lambda) = 0$ will be where the stability boundaries are located; i.e.,

$$\sigma^2 - 4\Lambda_{pq}\bar{\Lambda}_{qp} = 0. \tag{55}$$

Upon substitution of equations (44) and (51) into equation (55), the general pair of equations governing the stability boundaries is found to be

$$\epsilon = \pm \frac{2[\omega - (\omega_p + \omega_q)]}{\Omega_0 \sqrt{\omega_{pq}(\omega, p, q)}}, \tag{56}$$

where

$$\omega_{pq} = \tfrac{1}{4}\omega^2[(fs_{2p,2q-1} + fs_{2p-1,2q}) + \mathrm{i}(fs_{2q-1,2q-1} - fs_{2p,2q})][(fs_{2q,2p-1} + fs_{2q-1,2p})$$
$$- \mathrm{i}(fs_{2q-1,2p-1} - fs_{2q,2p})] + \tfrac{1}{2}\omega[(fs_{2p,2q-1} + fs_{2p-1,2q})$$

$$+ \mathrm{i}(fs_{2p-1,2q})][(fc_{2q-1,2p-1} - fc_{2q,2p}) + \mathrm{i}(fc_{2q,2p-1} + fc_{2q-1,2p})]$$

$$+ \tfrac{1}{2}\omega[(fc_{2p-1,2q-1} - fc_{2p,2q}) - \mathrm{i}(fc_{2p,2q-1} + fc_{2p-1,2q})][(fs_{2q,2p-1} + fs_{2q-1,2p})$$

$$- \mathrm{i}(fs_{2q-1,2p-1} - fs_{2q,2p})] + [(fc_{2q-1,2q-1} - fc_{2p,2q})$$

$$- \mathrm{i}(fc_{2p,2q-1} + fc_{2p-1,2q})][(fc_{2q-1,2p-1} - fc_{2q,2p}) + \mathrm{i}(fc_{2q,2p-1} + fc_{2q-1,2p})]$$

$$\text{for } p, q = 1, 2, 3, \ldots, m. \tag{57}$$

Equation (56) caters for all the possible sums of natural frequencies from all the m-modes of vibration. The dimensionless stability boundaries are plotted with ε versus ω. ω_{pq} of equation (57) will turn out to be a general real quadratic polynomial in ω because **FS** and

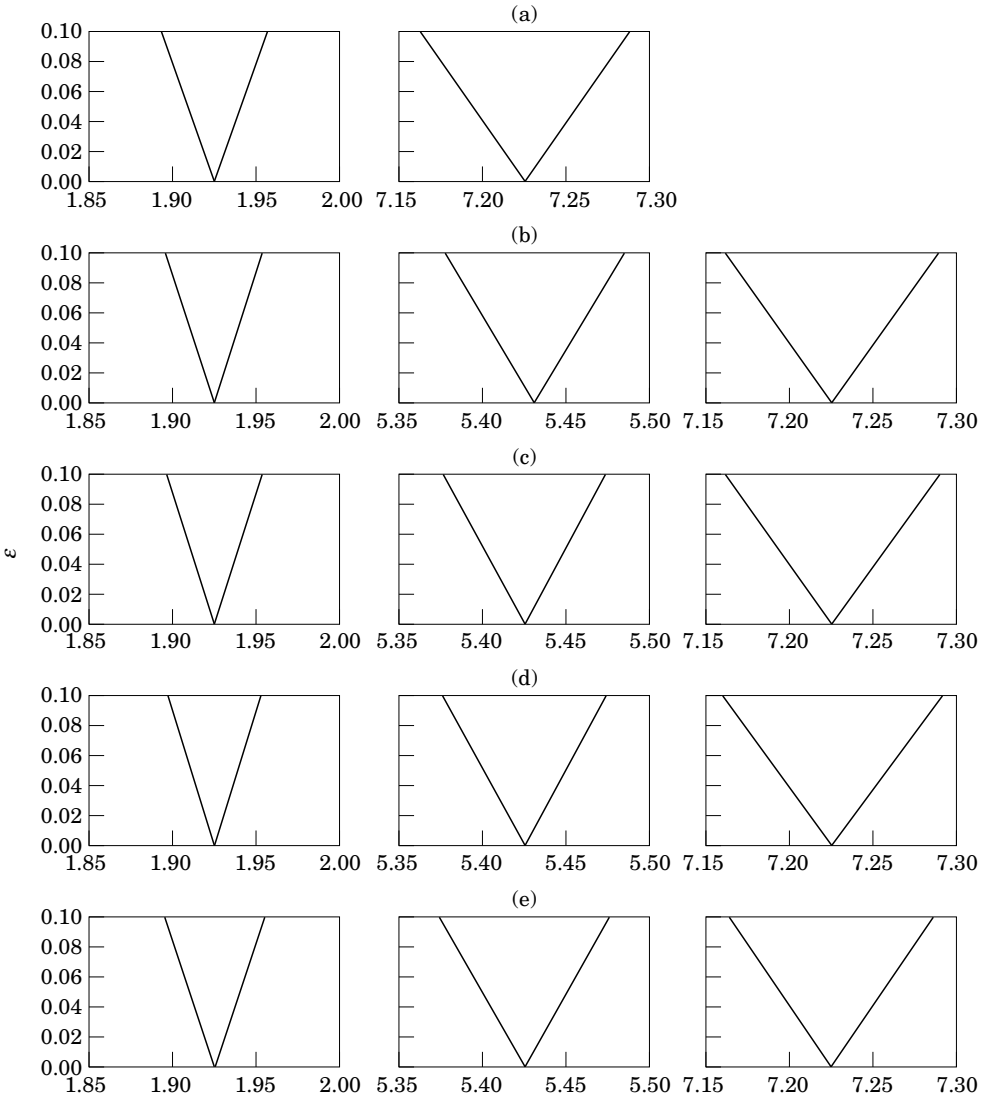

Figure 2. The convergent process of the first three unstable regions using $n = 1, \ldots, 5$ for a spinning Timoshenko beam ($\beta = 0{\cdot}15$) with $\Omega_0 = 50$. (a) $n = 1$; (b) $n = 2$; (c) $n = 3$; (d) $n = 4$; (e) $n = 5$.

FC consist of 2×2 blocks with zeros either on the diagonal or off-diagonal. The same finding was reported by Young and Liou [22].

3. RESULTS AND SIMULATIONS

In the present study, the dimensionless shaft parameters used in the numerical simulations are the Poisson ratio $v = 0{\cdot}3$ and the shear modulus. The circular cross-sectional area of the shaft, A, is computed from the radius of gyration r_0 defined by a non-dimensional parameter (Rayleigh's coefficient) $\beta = \pi r_0/L$.

Within the plotted array in each figure, all the individual plots have the same scale, to facilitate easy comparison of the width of their unstable regions. However, cross-comparison of subplots from different figures is invalid, due to the different scales used.

For this simply supported Timoshenko shaft, three-term ($n = 3$) assumed functions for V, W, Γ and B are found to be adequate for the convergence of spinning speeds for the boundaries of the first three unstable regions. This is illustrated in Figure 2, where all three unstable regions remain unchanged beyond $n = 3$. The shaft in Figure 2 has $\beta = 0{\cdot}15$ and $\Omega_0 = 50$.

The effect of the Rayleigh coefficient β, which relates the diameter of the shaft to its length, is first examined for the spinning shaft. The first three unstable regions for $\Omega_0 = 50$ are shown in Figure 3. Generally, all the unstable regions widen as β increases. However, the increase is more significant as β increases from 0·05 to 0·10 than from 0·10 to 0·15. Another observation made is the consistent right shift of almost all of the unstable regions. That is due to the increment of the various frequencies that constitute the pivoting ω-value of the unstable regions ($\omega = \omega_i + \omega_j$). The same trend is observed at other spin speeds.

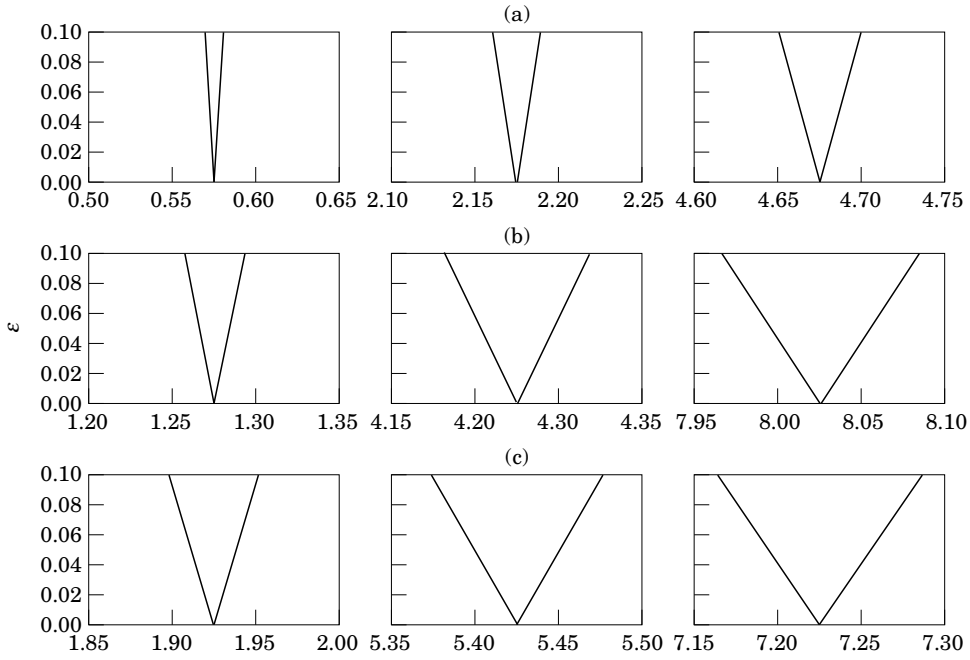

Figure 3. The first three unstable regions of three shafts with $\beta =$ (a) 0·05, (b) 0·10 and (c) 0·15, spinning at $\Omega_0 = 50$.

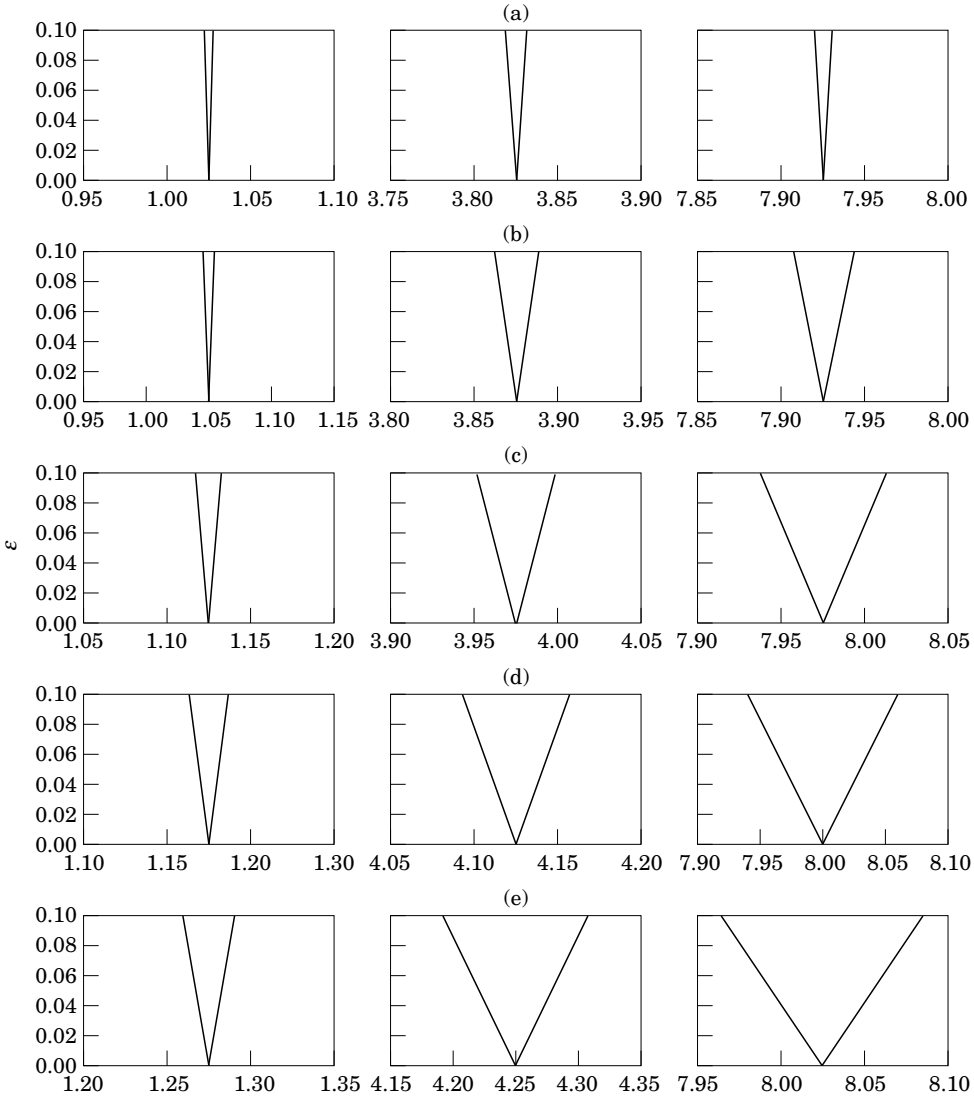

Figure 4. The first three unstable regions of the Timoshenko shaft ($\beta = 0{\cdot}15$) with Ω_0 = (a) 10, (b) 20, (c) 30, (d) 40 and (e) 50.

The effect of the steady state part of the dimensionless spin rate (Ω_0) is illustrated in Figure 4, in which $\beta = 0{\cdot}10$. It is apparent that the width of all the first three unstable regions undergoes a corresponding widening as the steady state spin rate (Ω_0) increases from 10 to 50, with an increment of 10. This near-linear width increment is in accordance with the fact that the undesirable gyroscopic moment is proportional to spin rate. Similar findings are also reported by Chen and Ku [27], who conclude that the gyroscopic moment has a destabilizing effect on rotating shafts. As in the case of increasing β, *all* of the subplots in Figure 4 are also observed to experience a right shift as Ω_0 increases.

A major advantage of this formulation is its simplicity. The present formulation, based on an inertial reference frame, results in a simpler form of equations of motion and the resulting characteristic equation for the stability analysis compared with that derived from

a body-fixed reference frame. Moreover, the boundaries of the unstable regions can easily be determined by evaluating **FS** and **FC** in equation (37) and subsequently substituting them into equation (56). It is also very interesting to note that **FS** and **FC** are made up of 2×2 blocks, with zeros either on the diagonal or off-diagonal. This in turn renders the ω_{pq} to be real quadratic polynomials in ω. The same result was obtained by Young and Liou [22]. All of the matrix computations involved can be carried out using any commercial package.

After obtaining the instability diagrams, various points near the unstable boundary, in and out of the unstable regions, are chosen. These parameter combinations are then substituted into equation (35) and integrated numerically for the time series of each b_i using *Mathematica* (capable of handling symbolic mathematics). It is verified that points in the unstable region are indeed unstable.

4. CONCLUSIONS

The equations of motion of a spinning Timoshenko shaft with a time-dependent spin rate have been formulated using Hamilton's principle and the assumed mode method in terms of an inertial reference frame. The time-dependent spin rate is assumed to be a steady state average value on which are superimposed sinusoidal perturbations. The multiple scales method is then employed to determine the primary regions of instability. Numerical results are presented for a simply supported spinning shaft. The sizes of the unstable regions are found to increase with a higher value of Rayleigh's coefficient, which relates the diameter of the shaft to its length. Most of the pivots of the unstable regions are found to encounter a right shift as Rayleigh's coefficient of the average spin rate increases. More importantly, the widths of the unstable regions are found to increase almost proportionally as the spin rate increases. This is due to the presence of the gyroscopic moment, which is proportional to the spin rate.

Discrepancies could have arisen due to the unsuitability of the Timoshenko beam being used on the beams, with too small a Rayleigh's coefficient.

REFERENCES

1. F. M. Dimentberg 1961 *Flexural Vibration of Rotating Shafts*. London: Butterworth.
2. V. V. Bolotin 1963 *Non-conservative Problems of the Theory of Elastic Stability*. New York: Macmillan.
3. R. G. Loewy and V. J. Piarulli 1969 *Dynamics of Rotating Shafts*. Washington, D.C.: The Shock and Vibration Information Center, Naval Research Laboratory.
4. R. L. Eshleman 1978 *Flexible Rotor Bearing System Dynamics*. New York: ASME Publications.
5. A. D. Dimarogonas and S. A. Paipeties 1983 *Analytical Methods in Rotor Dynamics*. New York: Applied Science.
6. J. S. Rao 1983 *Rotor Dynamics*. New York: John Wiley.
7. P. W. Likins, F. J. Barbera and V. Baddeley 1973 *American Institute of Aeronautics and Astronautics Journal* **11**, 1251–1258. Mathematical modeling of spinning elastic bodies for modal analysis.
8. H. F. Bauer 1980 *Journal of Sound and Vibration* **72**, 177–178. Vibration of a rotating beam, part 1: orientation in the axis of rotation.
9. R. M. Laurenson 1976 *American Institute of Aeronautics and Astronautics Journal* **14**, 1444–1450. Modal analysis of rotating flexible structure.
10. A. Y. T. Leung and T. C. Fung 1988 *Journal of Sound and Vibration* **125**, 523–537. Spinning finite elements.
11. C. P. Filipich, M. J. Maurizi and M. B. Rosales 1987 *Journal of Sound and Vibration* **116**, 475–482. Free vibrations of a spinning uniform beam with ends elastically restrained against rotation.

12. C. W. Lee and Y. G. Jei 1988 *Journal of Sound and Vibration* **126**, 345–361. Modal analysis of continuous rotor–bearing systems.
13. C. W. Lee, R. Katz, A. G. Ulsoy and R. A. Scott 1988 *Journal of Sound and Vibration* **122**, 119–130. Modal analysis of continuous rotor–bearing systems.
14. M. L. Chen and Y. S. Liao 1991 *Journal of Sound and Vibration* **147**, 497–513. Vibration of pre-twisted spinning beams under axial compressive loads with elastic constraints.
15. S. H. Choi, C. Pierre and A. G. Ulsoy 1992 *Journal of Vibration and Acoustics* **114**, 249–259. Consistent modeling of rotating Timoshenko shafts subject to axial loads.
16. J. W. Z. Zu and R. P. S. Han 1992 *ASME Summer Mechanics and Materials Meeting*, *April* 28–*May* 1, *Tempe*, *AZ*, **ASME 92-APM-6**, 1–8. Natural frequencies and mode shapes of a spinning Timoshenko's beam with general boundary conditions.
17. S. C. Huang and J. S. Chen 1990 *Journal of the Chinese Society of Mechanical Engineers* **11**, 63–73. Dynamic response of spinning orthotropic beams subjected to moving harmonic forces.
18. R. P. S. Han and J. W. Z. Zu 1992 *Journal of Sound and Vibration* **156**, 1–6. Modal analysis of rotating shafts: a body-fixed axis formulation approach.
19. E. Hashish and T. S. Sankar 1984 *Journal of Vibrations*, *Acoustics*, *Stress*, *and Reliability in Design* **106**, 80–89. Finite element and modal analyses of rotor–bearing systems under stochastic loading conditions.
20. T. R. Kane, R. R. Ryan and A. K. Banerjee 1987 *Journal of Guidance*, *Controls*, *and Dynamics* **10**, 139–151. Dynamics of a cantilever beam attached to a moving base.
21. D. C. Kammer and A. L. Schlack 1987 *Journal of Applied Mechanics* **54**, 305–310. Effects of non-constant spin rate on the vibration of a rotating beam.
22. T. H. Young and G. T. Liou 1992 *Transactions of the American Society of Mechanical Engineers*, *Journal of Vibration and Acoustics* **114**, 232–241. Coriolis effect on the vibration of a cantilever plate with time-varying rotating speed.
23. T. H. Young and G. T. Liou 1993 *Journal of Sound and Vibration* **164**, 157–171. Dynamic response of a rotating blade with time-dependent rotating speed.
24. C. L. Liao and B. W. Huang 1995 *International Journal of Mechanical Science* **37**, 423–439. Parametric instability of a spinning pretwisted beam under periodic axial force.
25. C. L. Liao and B. W. Huang 1995 *Journal of Sound and Vibration* **180**, 47–65. Parametric resonance of a spinning pretwisted beam with time-dependent spinning rate.
26. L. Meirovitch 1975 *Transactions of the American Society of Mechanical Engineers*, *Journal of Applied Mechanics* **42**, 446–450. A modal analysis for the response of linear gyroscopic systems.
27. L. W. Chen and D. M. Ku 1992 *Journal of Vibration and Acoustics* **114**, 326–329. Dynamic stability of a cantilever shaft–disk system.
28. A. H. Nayfeh *Nonlinear Oscillations*. New York: John Wiley.